Moderate static magnetic fields prevent estrogen deficiency-induced bone loss: Evidence from ovariectomized mouse model and small sample size randomized controlled clinical trial

Shenghang Wang[1,2☉], Jiancheng Yang[3☉], Yunpeng Wei[4], Chao Cai[2,5], Shuai Chen[2,5], Youde Wu[2,5], Xiao Li[2,5], Lilei Sun[2,5], Xianglin Li[2,5], Ming Gong[1], Jianhua Zhou[1], Yawei Hu[1], Wang Zhang[1], Zengfeng Guo[1], Jiacheng Liao[6], Chunling Luo[6], Xiaosu Bai[7], Xinle luo[1], Liming Duan[8], Ting Huyan[2,5], Zhouqi Yang[2,5], Min Wei[9], Yanwen Fang[9], Hao Zhang[1]*, Peng Shang (ID)[2]*

1 Department of Spine Surgery, People's Hospital of Longhua, Shenzhen, China, 2 Research & Development Institute of Northwestern Polytechnical University in Shenzhen, Shenzhen, China, 3 Department of Osteoporosis, Honghui Hospital, Xi'an Jiaotong University, Xi'an, China, 4 Shenzhen University of Advanced Technology, Shenzhen, China, 5 School of Life Sciences, Northwestern Polytechnical University, Xi'an, China, 6 Minle Community Health Service Center, People's Hospital of Longhua, Shenzhen, China, 7 Department of Endocrinology, People's Hospital of Longhua, Shenzhen, China, 8 An Shi Rui Information Technology Co., Ltd, Shenzhen, China, 9 Heye Health Technology Co., Ltd, Huzhou, China

☉ These authors contributed equally to this work.
* shangpeng@nwpu.edu.cn (PS); zhanghaodoctor1@hotmail.com (HZ)

🔓 OPEN ACCESS

Abstract

Background

Postmenopausal osteoporosis (PMOP) is the most common type of osteoporosis. Numerous studies have shown that static magnetic fields (SMFs) can inhibit bone loss by regulating bone remodeling. However, there are currently no clinical studies on the treatment of osteoporosis with SMFs. This study aims to investigate the clinical therapeutic effects of moderate static magnetic fields (MMFs) on PMOP.

Methods

In this paper, we constructed MMF device using neodymium-iron-boron (NdFeB) materials. At the animal level, the effect of MMF exposure for 8 weeks on estrogen deficiency-induced bone loss was investigated by evaluating bone microstructure, mechanical properties, and bone conversion using ovariectomized (OVX) mice. Clinically, a single-blind randomized controlled study in patients with PMOP was designed. PMOP patients aged 55–70 years were recruited and randomized into the control and MMF treatment groups. Clinical assessments of bone mineral density (BMD), bone turnover markers (BTMs) and VAS scores were performed at baseline and day 90, respectively.

Results

The results showed that MMF exposure significantly improved BMD, bone mineral content (BMC), bone microarchitecture and bone strength in OVX mice. For bone turnover, MMF increased the number of osteoblasts on the bone surface of OVX mice as well as the level of serum bone formation marker P1NP, while decreasing the number of osteoclasts and the level of serum bone resorption marker β-CTX. The clinical trial's results showed that MMF treatment had a positive effect on the improvement of BMD in the lumbar spine and increased serum P1NP levels while decreased β-CTX levels. In addition, MMF treatment decreased participants' VAS scores for low back pain.

Conclusions

The results of both animal and clinical studies demonstrated that MMF treatment improved bone turnover and have a positive effect on BMD improvement, as well as alleviated low back pain in PMOP patients. This study will promote the translational research and clinical application of SMF treatment for osteoporosis.

Trial registration

Intervention study of moderate static magnetic field on osteoporosis and iron metabolism in postmenopausal women, ChiCTR2100048604

Introduction

As the most common skeletal metabolic disease, osteoporosis (OP) is generally considered to be one of the factors contributing to the increased risk of fracture due to low bone mass and deterioration of bone microarchitecture [1]. Postmenopausal osteoporosis (PMOP) is caused by estrogen deficiency after women menopause, which is the most common type of age-related osteoporosis [2]. PMOP is a significant contributing factor to fractures in elderly women, and studies have indicated that the probability of fractures in women over the age of 50 is average up to 50% [3,4]. PMOP associated with population aging becomes a major clinical and public health problem.

Currently, medication is still the mainstay of osteoporosis treatment, with commonly used drugs including the anti-resorptive drugs such as bisphosphonates, denosumab, calcitonin, and selective estrogen receptor modulators, as well as the anabolic drugs such as teriparatide, romosozumab, etc. [5–7]. Physical therapy is an indispensable adjuvant therapy for the treatment of osteoporosis [8]. Electromagnetic field is an important treatment method for orthopedic diseases, and has been used for a long history spanning several decades. Pulsed electromagnetic field (PEMF) therapy has been approved for clinical adjunctive treatment of nonunion fractures and osteoporosis [9,10]. However, it still suffers from drawbacks such as high cost and limited portability.

Static magnetic fields (SMFs), as an easily obtainable physical factor, has been applied in the treatment research of orthopedic diseases for half a century [11–13]. Compared to other types of electromagnetic fields such as PEMF and radiofrequency electromagnetic fields (RFs), SMFs exhibit higher biosafety due to its passive nature and energy-free. Moderate static magnetic fields (MMFs) refer to SMFs with a magnetic induction intensity between 1mT and 1T, which could be acquired by permanent magnetic materials such as Samarium-Cobalt and Neodymium, which allow wide applicability at an affordable price [14,15]. Various studies have demonstrated that MMFs could promote repair of fracture and bone defect, and inhibit bone loss, by modulating the physiological functions of osteoblast, osteoclast, and osteocyte [16,17]. The intramedullary implant with MMFs could improve fracture healing in rabbits [18,19]. Our preliminary research found that 0.2–0.4 T MMF whole-body exposure alleviated bone loss in OVX mice [20]. However, the clinical effectiveness of SMFs in the treatment of osteoporosis remains a mystery.

To figure out the therapeutic effectiveness and potential applications of MMFs in PMOP, we evaluated the effect of MMF on bone loss in ovariectomized (OVX) mice at the animal level; and designed a small sample size randomized controlled trial (RCT) to investigate the therapeutic efficacy of MMF on osteoporosis in postmenopausal women at the clinical level.

Methods

Clinical trial design

A randomized single-blind trial was conducted in People's Hospital of Longhua between July 21st 2021 and April 18th, 2023. This clinical trial was performed in accordance with the approved institutional ethical protocol (Ethical Review of People's Hospital of Longhua [2021] No.106) and registered in the "Chinese Clinical Trial Registry (ChiCTR)" (ChiCTR2100048604). All procedures will be performed according to the Declaration of Helsinki. All individuals were signed the informed consent from providing their written consent prior to participation after being advised, verbally and written, of the objectives, risks, and benefits of the study.

Participants. Postmenopausal women with osteoporosis (diagnosed by dual energy X-ray absorptiometry, T score ≤−2.5), aged between 55 and 70 years, were recruited in this study by advertisement, self-referral, or physician referral at People's Hospital of Longhua (Shenzhen, China). Patients with the following criteria were excluded: (i) Prior spine surgery; (ii) Had taken fracture within 6 months before enrolment; (iii) Had taken Glucocorticoids, estrogen, or diuretic drugs within 6 months before enrolment; (iv) Had taken drugs affecting bone metabolism within 6 months before enrolment, excluding calcium agents and ordinary vitamin D; (v) Other diseases that affect bone metabolism, including thyroid disease, osteomalacia, rheumatoid arthritis, tumor, cushing's disease, diabetes, etc.; (vi) Uterus or ovaries removed; (vii) Heart disease, or implantable pacemaker wearer; (viii) BMI ≥ 28; (ix) Hematological system diseases; (x) Abnormal liver and kidney function (Deviation of indicators by more than twice the normal value); (xi) Alcoholism or drug abuse.

Sample size was calculated (G*Power 3.1.9, Christian-Albrechts-Universitat, Kiel, Germany) using areal bone mineral density (aBMD) of as the primary outcome, $\alpha = 0.05$, and power of 80% for between-group analysis. Considering a mean difference of 0.1 and a standard deviation of 0.07 in the mean aBMD between groups, sample size was estimated as 9 individuals per group. However, to account for losses during the follow-up period, the final sample size was 30 participants (15 per group).

Interventions. The workflow of study was outlined in Fig 1. Clinical evaluation was performed by orthopaedic surgeons. Briefly, the participants were randomized into two groups: Control group and MMF group. Specifically, a series of random numbers were generated on SPSS software with a seed number set by a statistician (who did not participate in the inclusion of cases and experimental research processes), where every 2 random numbers formed a block. The participants were assigned to the corresponding groups in chronological order of enrollment. The grouping table is kept by the statistician and strictly confidential. Participants will be blinded since they will not know the exercise performed in the other group, and interventions will be performed individually. Participants in the MMF group were instructed to wear
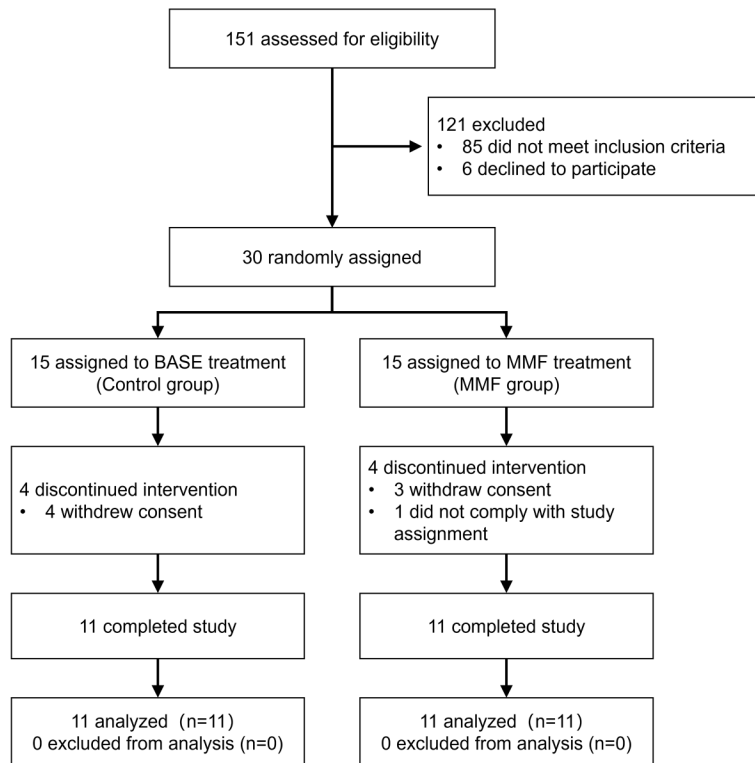
Fig 1. Flowchart of the clinical trial.

https://doi.org/10.1371/journal.pone.0314199.g001

a waist belt containing the MMF device (Fig 2) for 6 hours each day, five days a week. The wearable MMF device was composed of NdFeB, with the same array as the MMF exposure device for mice, which ensured that the participants' lumbar vertebrae (L1-L4) exposed to MMF (>1 mT) during the wearing process (Fig 2C-E). The relative position between the device and the participants during the wearing process was showed as Fig 2F. To avoid interference from placebo effects, the belt without MMF have been conducted, with the appearance, material, and weight same as wearable MMF device. Participants in the control group were instructed to wear the waist belt without MMF for 6 hours each day, five days a week. All participants received calcium (1200 mg), calcitriol (50 μg), and salmon calcitonin (20 μg) once daily as a basic treatment. The entire experimental process lasted for 90 days

Procedures. Participants' characteristics (age, body mass, height, body mass index, and age of menopause) were collected at baseline assessment. Primary and secondary outcomes were measured at the baseline assessment, immediately after the 90 days intervention period. The primary outcomes were areal bone mineral density (aBMD) of the lumbar spine, total hip, and femoral neck, as well as the Visual Analogical Scale (VAS) of Low Back Pain. The secondary outcomes were serum bone turnover markers levels.

BMD analysis. aBMD of the lumbar spine, total hip, and femoral neck were assessed at 0 and 3 months by dual x-ray absorptiometry (DXA) using a Hologic QDR 4500A densitometer (Hologic, Waltham, MA, USA). The coefficients of variation for DXA repeated measurements of the lumbar spine, total hip, and femoral neck were 0.7%, 1.4%, and 1.9%, respectively.

Biochemical analysis. Fasting morning blood samples were obtained at 0 and 3 months. Serum bone formation markers P1NP and OCN as well as the bone resorption marker β-CTX were measured using the Au-400 automated biochemical analyzer (Olympus, Tokyo, Japan).
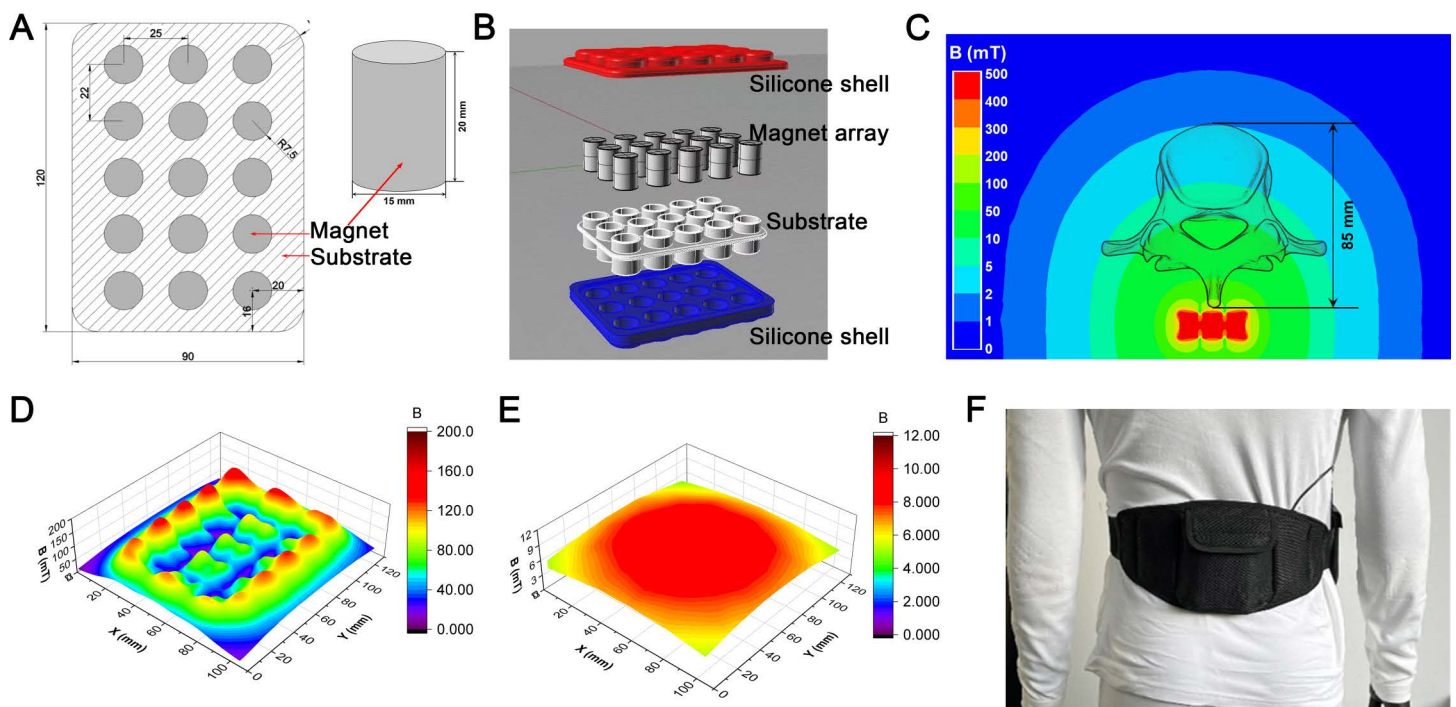
Fig 2. Moderate static magnetic field (MMF) device in clinical trial. (A) Schematic diagram of magnet size and array layout of MMF device. (B) Magnetic packaging structure. (C) The magnetic field distribution of vertebrae during MMF exposure was simulated using ANSYS software. (D, E) Magnetic field distribution at 5 mm (D) and 90 mm (E) above the magnet were measured by MIST magnetic field space-time imaging system. (F) Diagram of the body-worn MMF device.

https://doi.org/10.1371/journal.pone.0314199.g002

Visual Analogical Scale (VAS) of low back pain. The participants were asked to express the intensity of the perceived low back pain (lumbar pain) on a one-dimensional scale. The scale was divided into 10 equal segments to represent distinct levels of pain. At one end, labeled as 0, participants indicated the absence of pain, while at the other end, labeled as 10, they expressed the highest imaginable level of pain [21].

Monitoring system of wearable state of MMF device

To evaluate the daily wearing time of the participants during the clinical trial, a corresponding real-time monitoring and statistical system was constructed. The hardware components of the monitoring system consisted of sensors, signal generation module with power supply (Fig S1A and B in S1 Data). The sensors were capable of collecting information about the wearing state at intervals of every 15 seconds, including parameters such as temperature and respiration. Subsequently, the sensors transmitted the collected information to the signal generation module, further uploading it to the cloud-based monitoring system's backend software utilized 4G signals (Fig S1D B in S1 Data). Researchers were able to observe the participants' wearing status of the device in real-time through the monitoring cloud platform and perform statistical analysis on wearing time (Fig S1E and F B in S1 Data). The wearable device monitoring system was not only designed to enhance data validity, but also to enable researchers to remind participants about wearing the devices, thereby promoting participant compliance.

Animals and Treatments

Twenty-four adult ten-week-old female C57BL/6 mice were housed at an ambient temperature of 25°C under an artificial 12 h light/dark cycle with food and water provided. All experiment mice were randomly divided into three groups: Control

group, OVX group, OVX-MMF group. After anesthesia with isoflurane, mice in OVX group and OVX-MMF group were ovariectomized, and the fat around the ovaries were excised in the mice of control group. Mice in OVX-MMF group were housed with the bottom of their cages equipped with moderate static magnetic field device. While cages of mice in OVX group were equipped with the same structural devices but without MMF.

After two weeks of the operation, the mice were treatment with MMF for 8 weeks, continuously. At the end of the eight-week treatment, the mice were euthanized by cervical dislocation under anesthesia. The blood samples and organs were collected for subsequent analyzes. All animal protocols used in this study were approved by the Lab Animal Ethics and Welfare Committee of Northwestern Polytechnical University (No.202101102).

MMF exposure device for mice

MMF exposure device for mice is composed of a plurality of N42 neodymium-iron-boron (NdFeB) magnet. Each magnet particle has a diameter of 15 mm and a height of 20 mm. The arrangement of pairs between particles and the relative position of mice during exposure to MMF are shown in Fig 3A and 3B. The magnetic induction intensity on the device and 1 cm away from the device was measured by MIST magnetic field space-time imaging system (Eastforce Superconducting Technology Co., Ltd, Beijing, China), and ranged from 20 mT to 100 mT (Fig 3C). The direction of magnetic induction lines is shown in Fig 3D.

BMD and BMC examination

After eight weeks treatment, all mice were anesthetized and placed in a Dual-energy X-ray scanner (InAlyzer; MEDIKORS, Korea) to measure bone mineral density (BMD) and bone mineral content (BMC), including total body, femur, tibia and lumbar vertebrae.

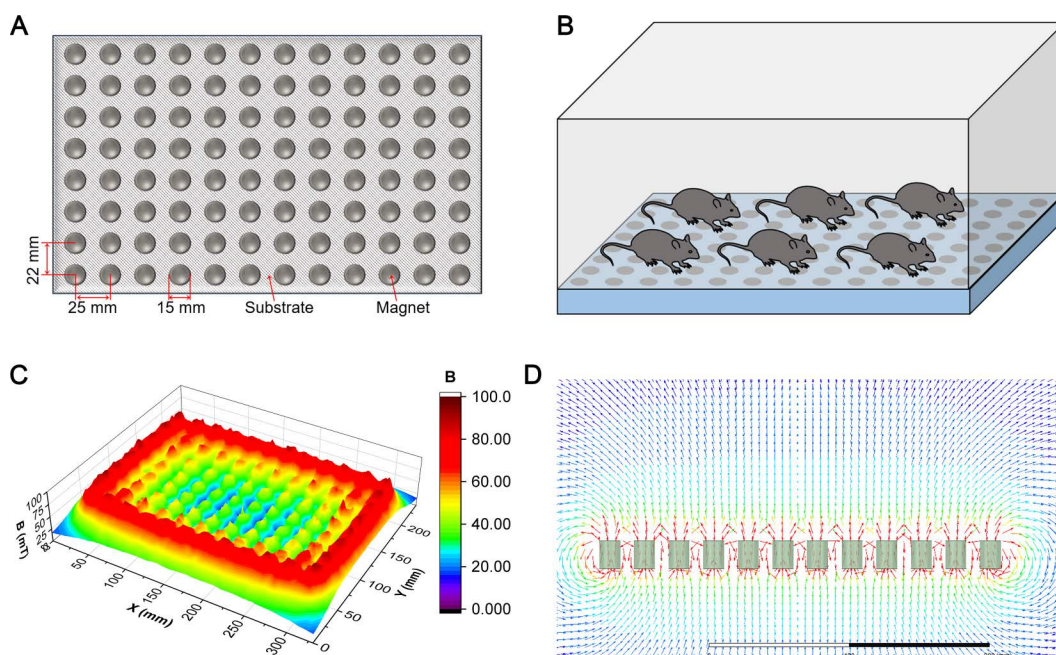**Fig 3. Moderate static magnetic field (MMF) exposure device for mice.** (A) The diagram of magnetic plate that provide MMF. (B) Relative position of mice during exposure to MMF. (C) Magnetic field distribution in the mouse exposure area, 1 cm above the magnetic plates. (D) Direction and distribution of magnetic induction lines in magnetic exposure systems.

https://doi.org/10.1371/journal.pone.0314199.g003

Bone microarchitecture examination

The left femur and lumbar vertebrae of mice were used for bone microarchitecture detection by a high-resolution micro-CT scanner (VivaCT80, SCANCO Medical AG, Bassersdorf, Switzerland). Scanning was performed at 70 kV, 114μA, 250ms without a filter. During the microstructure analysis of femur, area-of-interest (ROI) of 1-mm-long from the distal growth plate 0.5 mm to 1.5 mm were defined for analysis of trabecular bone, and another 1-mm-long ROI from the distal growth plate 5 mm to 6 mm were selected for analysis of cortical. Meanwhile, the trabecular bone in the L4 lumbar vertebrae were analyzed to evaluate the impact of the MMF exposure on bone loss in lumbar vertebrae. For the assessment of vertebral trabecular bone, the ROI was established within 0.5 mm from the edge of the cortical bone.

The parameters of the ROI were three-dimensionally reconstructed using Scanco analysis software (SCANCO Medical AG, Bassersdorf, Switzerland) to analyze trabecular structural parameters including bone volume fraction (BV/TV), trabecular number (Tb.N), trabecular thickness (Tb.Th), trabecular separation (Tb.Sp), BMD; and cortical bone structural parameters including cortical thickness (Ct.Th), cortical area (Ct.Ar), cortical area fraction (Ct.Ar/Tt.Ar), cortical porosity (Ct.Po), and tissue mineral density (TMD).

Bio-mechanical examination

The left tibia was placed on two support points spaced 10 mm apart in a material mechanics machine, and then the upper loading device was perpendicular to the center of the tibia and moved downward at a rate of 1 mm/min to complete the three-point bending test. The inner and outer diameters of the long and short axes of the tibial fracture surface were measured by Digital Microscope KH-8700 (HIROX, Japan). Then, the computer-generated load-displacement curves and the stress-strain curve were analyzed to assess the mechanical properties of the tibia, including stiffness, ultimate load, ultimate stress, elastic modulus, bending energy absorption.

Take the L3 lumbar vertebra, remove the soft tissue on both sides, and use axial compression to test the mechanical properties of the vertebrae. The loading device was positioned perpendicular to the vertebral cross-section and moved downward at a rate of 1 mm/min. Then, the computer-generated load-displacement curves and the stress-strain curve were analyzed to assess the mechanical properties of the vertebrae, including stiffness, ultimate load, and elastic modulus.

Histochemical analysis

After the bone microstructure examination, the femur was collected and soaked in 10%EDTA with a PH of 7.5 and decalcified at 4 °C for two weeks, during which the decalcified fluid was changed every three days. The decalcified femur was embedded in paraffin and cut into 5mm thick sections using a semi-automatic rotary microtome (Leica Biosystems RM2245, Germany). Osteoblasts were observed by hematoxylin and eosin staining (H&E; Beyotime Biotechnology, Shanghai, China). Osteoclasts were identified by tartrate-resistant acid phosphatase staining (TRAP; Sigma-Aldrich, USA). The images of bone sections were acquired by Nikon 80i microscope (Nikon, Japan). Osteoblastogenesis was evaluated by analyzing osteoblast number per bone surface (N.Ob/BS), and osteoclastogenesis was estimated by quantizing osteoclast number per bone surface (N.Oc/BS) and osteoclast surface per bone surface (Oc.S/BS) by using Image-J software.

Biochemical analysis

The blood samples were collected through cardiac puncture and centrifuged at 1000g for 10 min to obtain serum. Bone turnover markers (BTMs), including propeptide of type I procollagen (P1NP), osteocalcin (OCN), and beta-isomer of the C-terminal telopeptide of type I collagen (β-CTX) were detected by ELISA kit (JiangLai biological, Shanghai, China). All procedures are performed in accordance with the kit instructions.

Statistical analysis

The normally distributed continuous data will be expressed as mean ± standard deviation (SD), as median (IQR) for endpoints without a normal distribution. The data about mean aBMD percentage change in clinical will be expressed trial as mean ± standard error (SE), as per the reporting conventions for this study area. The normal distribution was tested by Kolmogorov-Smirnov test with $P > 0.10$. The comparison of group differences in normally distributed continuous data was performed using t-tests or ANOVA. Non-parametric rank-based tests were employed for the comparison of group differences in non-normally distributed continuous data. The comparison of group differences in categorical data was conducted using the chi-square test, and Spearman's rank correlation analysis was employed to assess the correlation between variables. $P < 0.05$ will be considered to be statistically significant. To minimize the risk of Type I errors, the primary and secondary outcomes in the clinical trial were adjusted using the Holm-Bonferroni correction, respectively. To assess the risk of false negatives in the clinical trial, post-hoc power analysis will be conducted on the results that did not show statistical significance. All the statistical data will be analyzed by GraphPad Prism (version 8; GraphPad Software, Inc., San Diego, CA, USA).

Results

Effects of MMF exposure on bone quality in OVX mice

The body weight of mice was measured every four days, and there was no statistically significant difference in body weight among the different groups (Fig S2B in S1 Data). The effects of MMF exposure on BMD and BMC in OVX mice were detected by DXA and shown in table S1 B in S1 Data. The results showed that the OVX decreased the BMD and BMC in mice. The MMF exposure increased BMD of the total body, femur, and lumbar vertebrae in OVX mice. Meanwhile, the femoral BMC and lumbar vertebral BMC in OVX mice were significantly increased by MMF exposure. While, there was no significant difference in the tibial BMD, total BMC, and tibia BMC in OVX-MMF group compared to OVX group.

Micro-CT scanning of the femur was used to evaluate effects of MMF exposure on the microstructure of weight-bearing bones in OVX mice. Representative three-dimensional imaging of cortical bone and trabecular bone were illustrated (Fig 4A and B). In cortical bone of femoral mid-shaft, the results showed OVX significant decreased Ct.Th, Ct.Ar, Ct.Ar/Tt.Ar and TMD, while markedly increased Ct.Po. Furthermore, Ct.Ar/Tt.Ar was significantly increased in OVX-MMF group compared to the OVX group (Fig 4C). For the trabecular bone of distal femur, OVX group showed significant decreases in BV/TV, Tb.N, Tb.Th and BMD, whereas significant increases in Tb.Sp. compared with the control group. Compared to the OVX group, MMF exposure significantly increased BV/TV, Tb.N, Tb.Th, and BMD, while decreased Tb.Sp in trabecular bone of the distal femur (Fig 4D). In conclusion, these data suggested that MMF exposure ameliorates OVX-induced structural destruction of cortical bone and trabecular bone in the femur. Micro-CT scanning on the lumbar vertebra was used to evaluate the effect of MMF exposure on the microstructure of non-weight-bearing bones. Representative three-dimensional imaging of lumbar vertebra was illustrated in Fig S3A B in S1 Data. The statistical results showed that OVX decreased the BMD, BV/TV, Tb.N, and Tb.Th, while increased the Tb.Sp in mice. MMF exposure increased the BV/TV, Tb.Th, and BMD, while decreased the Tb.Sp of lumbar vertebra in OVX mice (Fig S3B in S1 Data).

Three-point bending was used to evaluate changes in the mechanical properties of the tibia. The results exhibited stiffness, ultimate load, ultimate stress, elastic modulus, and bending energy absorption were significantly decreased in OVX group. Compared with the OVX group, the MMF exposure restored the stiffness, ultimate load, and bending energy absorption of tibia. Whereas, there was no significant differences in ultimate stress and elastic modulus between mice in OVX group and OVX-MMF group (Fig 4E). The axial compression test was used to evaluate changes in the mechanical properties of the lumbar vertebra. The results showed that stiffness, elastic modulus, and ultimate load of lumbar vertebra were significantly reduced after OVX, but MMF exposure significantly increases the values of these parameters (Fig. S3C, B in S1 Data). These results suggested that MMF exposure significantly repairs the weakening of bone strength caused by OVX.
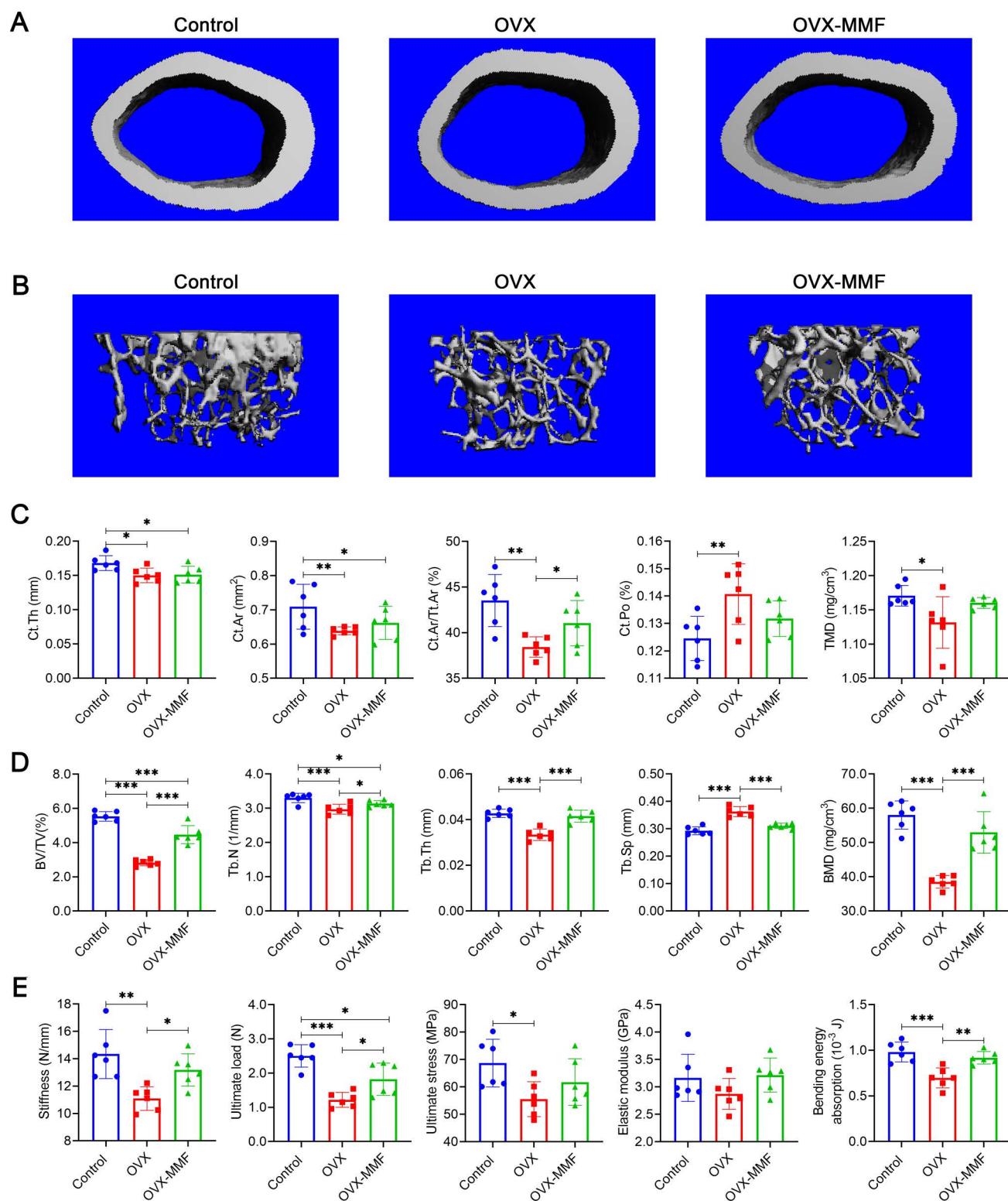
Fig 4. Effects of MMF exposure on bone structure and mechanical properties in OVX mice. (A) Three-dimensional images of cortical architecture in femoral mid-shaft by micro-CT scanning. (B) Three-dimensional images of trabecular architecture in distal femur by micro-CT scanning. (C) Structural

parameters of cortical bone, including Ct.Th, Ct.Ar, Ct.Ar/Tt.Ar, Ct.Po, and TMD. (D) Structural parameters of trabecular bone, including BV/TV, Tb.N, Tb.Th, Tb.Sp, and BMD. (E) Mechanical properties of the tibia in mice were detected through the three-point bending test, including stiffness, ultimate load, ultimate stress, elastic modulus, and bending energy absorption. n = 6. *$P < 0.05$, **$P < 0.01$, ***$P < 0.001$.

Effects of MMF exposure on bone turnover in OVX mice

Bone formation is mainly mediated by osteoblasts, and bone resorption is mainly mediated by osteoclasts. The osteoblastogenesis and osteoclastogenesis were detected by H&E and TRAP staining in femur. The distribution of osteoblasts on the surface of cortical bone and trabecular bone were displayed in Fig 5A. The statistical results showed OVX decreased the N.Ob/BS of trabecular bone and cortical bone. Statistical comparisons demonstrated that MMF exposure for 8 weeks significantly increased the N.Ob/BS of trabecular bone, while have no significant effect on the N.Ob/BS of cortical bone compared with the OVX mice without MMF exposure (Fig 5B, C). The OVX treatment reduced the levels of OCN and P1NP in the serum of mice, and the MMF exposure increased the P1NP content in OVX mice (Fig 5D, E). The distribution of osteoclasts on the surface of cortical and trabecular bone were displayed in Fig 5F. Statistical results demonstrated OVX increased the N.Oc/BS and OC.S/BS of trabecular bone and cortical bone. MMF exposure could significantly decreased the N.Oc/BS and OC.S/BS of cortical and trabecular bones in OVX mice (Fig 5G-J). Serum biochemical analysis showed that MMF exposure significantly decreased bone resorption markers β-CTX compared with the OVX group (Fig 5K).

Baseline characteristics of subjects in clinical trial

A RCT was implemented to initially and exploratively evaluate the efficacy of MMF in PMOP. As shown in Fig 3, 30 subjects were ultimately enrolled in the clinical trial. During the course of the trial, 8 cases withdrew from the trial, of which 7 cases (4 cases in the control group and 3 cases in the MMF group) voluntarily withdrew their consent and 1 case (in the MMF group) did not comply with the study procedures. No participants reported any adverse events throughout the clinical trial. The baseline characteristics of the 22 subjects who persisted to the trial endpoint were showed in Table 1. Participants in both groups had similar baseline characteristics, including age, age at menopause, height, weight, BMI, serum BTMs, and VAS scores of low back pain.

Effects of MMF wearable device treatment on bone mineral density of subjects in clinical trial

After 90 days treatment, the aBMD of lumbar spine, total hip, and femoral neck of participants were tested by DXA and showed in table S2B in S1 Data. The statistical data showed that the lumbar spine aBMD had increased by 1.88% (SE 1.39 [CI −1.22–4.99]) from baseline in the control group, by 2.86% (SE 1.41 [CI −0.27–5.99]) in the MMF group (Fig 6A). The total hip aBMD had increased by 0.09% (SE 1.11 [CI −2.38–2.56]) from baseline in the control group, by 2.37% (SE 1.09 [CI −0.06–4.81]) in the MMF group (Fig 6B). The femoral neck aBMD had increased by 1.29% (SE 1.69 [CI −2.47–5.05]) from baseline in the control group, by 2.96% (SE 1.27 [CI −0.12–5.79]) in the MMF group (Fig 6C). However, there were no statistically significant changes on aBMD at the lumbar spine, total hip, and femoral neck of participants in MMF treatment (MMF group) compared with non-MMF exposure (control group). Additionally, the post-hoc power analysis showed that the post-hoc power of aBMD of lumbar spine, total hip, and femoral neck were 0.075, 0.28, and 0.116, respectively. The results of the repeated-measures ANOVA showed that the aBMD of lumbar spine in all participants exhibited a significant time effect (P = 0.02), but there was no significant interaction between time and group (P > 0.05). Additionally, significant individual variations were observed in the changes of aBMD of lumbar spine, total hip, and femoral neck (P < 0.001). Furthermore, we analyzed the relationship between the lumbar aBMD of participants and their age. The enhancing effect of MMF treatment on aBMD had a higher negative correlation with participants' age compared to the control group (Fig S4B in S1 Data).
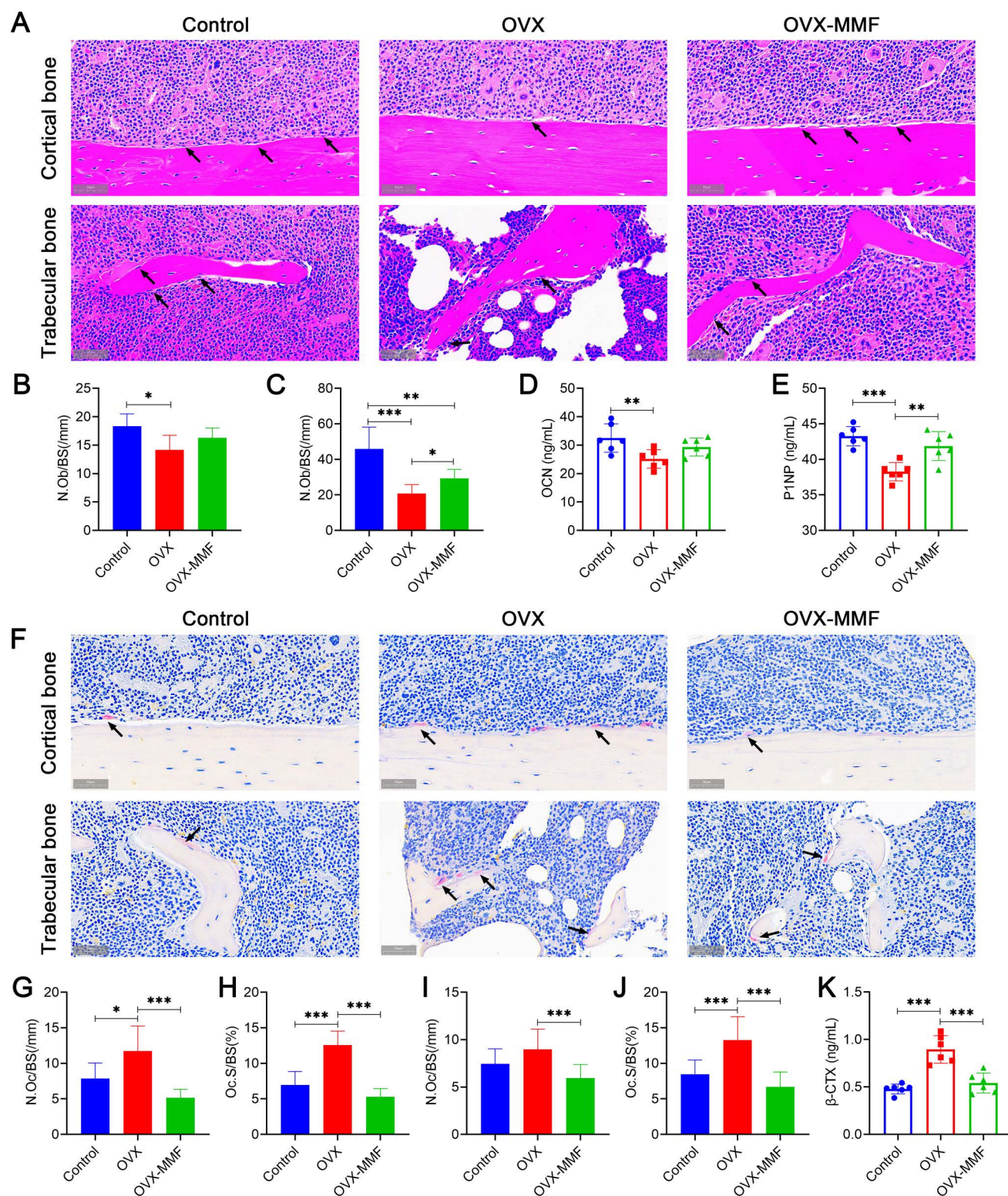
Fig 5. Effects of MMF exposure on bone remodeling in OVX mice. (A) H&E staining of cortical bone in femoral mid-shaft and trabecular bone in distal femur (Scale bar = 100 μm). Black arrows mark osteoblasts. (B) The osteoblast number per bone surface (N.Ob/BS) in cortical bone. (C) The

osteoblast number per bone surface (N.Ob/BS) in trabecular bone. Serum bone formation markers, OCN **(D)** and P1NP **(E)** were detected using the commercial ELISA kits. (F) TRAP staining of cortical bone in femoral mid-shaft and trabecular bone on distal femur (Scale bar = 100 μm). Osteoclast number per bone surface (N.Oc/BS) **(G)** and osteoclast surface per bone surface (Oc.S/BS) **(H)** in cortical bone. osteoclast number per bone surface (N.Oc/BS) **(I)** and osteoclast surface per bone surface (Oc.S/BS) **(J)** in trabecular bone. (K)Serum bone resorption marker, β-CTX was detected using the commercial ELISA kit. n = 6. *$P < 0.05$, **$P < 0.01$, ***$P < 0.001$.

https://doi.org/10.1371/journal.pone.0314199.g005

Table 1. Participants baseline characteristics.

	BASE treatment /Control group (n = 11)	MMF treatment /MMF group (n = 11)
Age (years)	64.45 ± 5.18	61.82 ± 5.69
Age of menopause (years)	50.45 ± 3.62	48.45 ± 2.66
Body-mass index (kg/m²)	22.14 ± 2.09	21.95 ± 1.61
Areal bone mineral density (g/cm²)		
Lumbar spine	0.724 ± 0.098	0.743 ± 0.077
Total hip	0.708 ± 0.069	0.693 ± 0.077
Femoral neck	0.631 ± 0.063	0.621 ± 0.066
Bone turnover markers		
Serum OCN (μg/L)	22.42 ± 6.39	20.99 ± 8.19
Serum P1NP (μg/L)	65.23 ± 32.44	59.38 ± 26.21
Serum β-CTX (ng/L)	384.7 ± 204.5	423.2 ± 300.2
VAS	3.54 ± 1.64	3.18 ± 1.94

Data are shown in mean ± SD. OCN = osteocalcin. P1NP = N-propeptide of type 1 procollagen. β-CTX = beta-isomer of the C-terminal telopeptide of type I collagen. VAS = visual analogical scale of low back pain

https://doi.org/10.1371/journal.pone.0314199.t001

Effects of MMF treatment on bone turnover markers and low back pain of subjects in clinical trial

After 90 days treatment, BTMs level of participants were showed in table S2 B in S1 Data. Compared to the control group, levels of the bone formation marker OCN decreased more in the MMF group (−22.87% [CI −16.31–3.15]*vs* −6.58% [CI −32.07–−13.67], *P* = 0.0135) (Fig 7A). The levels of P1NP showed a lesser decrease in MMF group than the control group (−14.54% [CI −40.16–−23.57] *vs* −31.86% [CI −25.17–−3.91], *P* = 0.0096) (Fig 7B). The level of bone resorption marker β-CTX increased by 4.85% [CI −33.58–−43.27] from the baseline value in the control group (Fig 7C). In contrast, β-CTX levels decreased by 38.83% [CI −59.69–−17.97] from the baseline value in the MMF group. Furthermore, the rate of β-CTX change in the MMF group showed a significant difference when compared to the control group (*P* = 0.0377).

Due to the presence of symptoms of low back pain among some participants, the VAS score was employed to assess the participants' low back pain before and after the treatments. The results showed that VAS scores were significantly lower in the MMF group compared to the control group (−2.800 [CI −2.25–−0.11] *vs* −1.182 [CI −3.46–−2.14], *P* = 0.0114), suggesting that MMF treatment relieved low back pain of participants (Fig 7D).

Discussion

MMFs have been used in orthopedics diseases studies for over half a century. In this study, we performed a first clinical trial to evaluate the effects of MMF on PMOP. Although this study was a small sample size RCT, the preliminary results demonstrated the effectiveness of MMF exposure for PMOP therapy, including reduced bone turnover and alleviated low back pain.

As a chronic and progressive disease, the treatment of PMOP typically requires several years and may even extend throughout a patient's lifetime [22,23]. Therefore, the compliance of patients is crucial for the effectiveness of osteoporosis therapy [24,25]. In order to improve patient compliance, we conducted a wearable MMF device which could be carried by
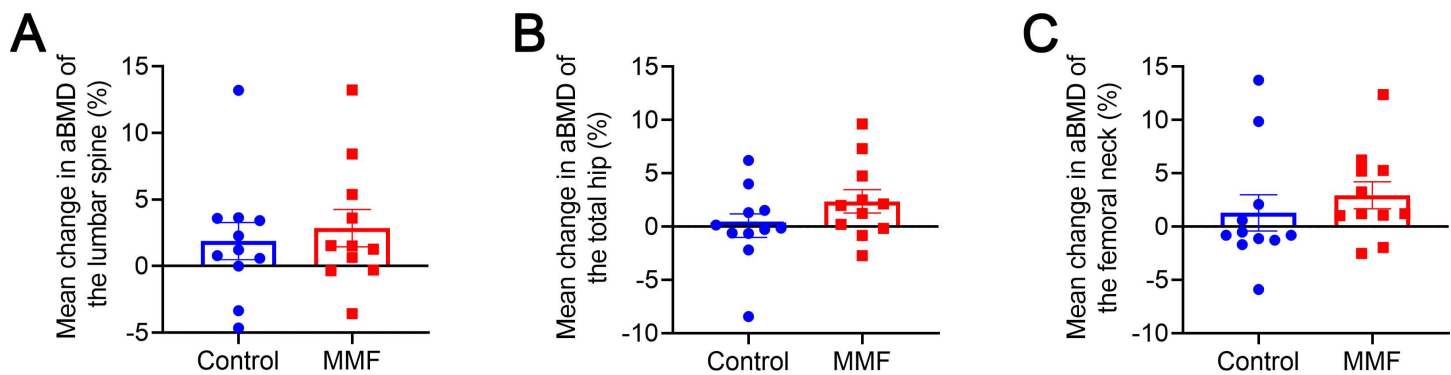
Fig 6. Mean percentage change in aBMD of the lumbar spine (A), total hip (B), and femoral neck (C) after 90 days treatment in clinical trial. aBMD = areal bone mineral density.

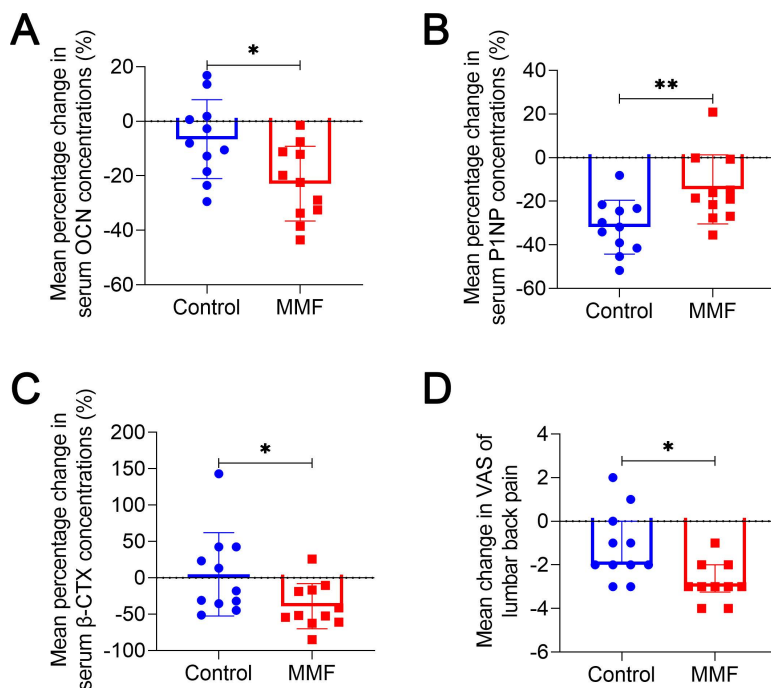https://doi.org/10.1371/journal.pone.0314199.g006

Fig 7. Change in bone turnover markers and VAS of low back pain after 90 days treatment in clinical trial. (A-C) Mean percentage change in serum concentrations of bone formation makers, OCN (A) and P1NP (B), as well as bone resorption marker β-CTX (C). (D) Mean change in VAS of low back pain after 90 days treatment in clinical trial. OCN = osteocalcin. P1NP = N-terminal propeptide of type 1 procollagen. β-CTX = beta-isomer of C-Terminal Telopeptide of Type I Collagen. *$P < 0.05$, **$P < 0.01$.

https://doi.org/10.1371/journal.pone.0314199.g007

the patients themselves, and allowing them to complete the trial in their own homes. However, home-based trial without the presence of researchers cannot guarantee participants' adherence to the designated trial procedures. Therefore, sensors were incorporated into the device to monitor the participants' wearing status in real-time.

BMD is the gold standard for evaluating the impact of interventions on bone loss. In this study, we assessed the effect of a MMF device on BMD in OVX mice and evaluated its therapeutic efficacy in preventing postmenopausal osteoporosis through a clinical trial. The results showed that the continuous MMF exposure for 8 weeks significantly

increased BMD and microstructure of the femur and lumbar vertebrae in OVX mice. The participants in control and MMF group demonstrated a well compliance, and no adverse reactions were observed in clinical trial. The results of the repeated-measures ANOVA showed that aBMD of lumbar spine significantly increased in both groups after the 90-day intervention. Meanwhile, the results indicated that although there was no statistically significant difference in the improvement of aBMD of lumbar spine, total hip, and femoral neck between the MMF group and the control group, the MMF treatment demonstrated a greater magnitude of increase in aBMD in PMOP patients. Additionally, the results of the post-hoc power analysis showed that the statistical powers of aBMD of lumbar spine, total hip, and femoral neck were low, all being less than 0.5. This indicates a high risk of false negatives in the statistical results for change of aBMD. Additionally, the statistical results showed significant individual variations in the changes of aBMD among the participants. Due to the small sample sizes in both the control and experimental groups in this clinical trial, individual variability could be one of the major reasons for the low statistical power. Bone mineral density changes are typically a gradual process, and the short duration (90-day interval) of repeated measurements may not have been sufficient to fully capture the effects of MMF on bone mineral density. Therefore, the future clinical research on the effects of SMFs on PMOP should consider designing larger-scale and longer trial periods to further investigate the potential impact.

The results of clinical trial showed that all two treatments approaches exhibited a decrease in the concentration of bone formation and bone resorption markers in serum. The MMF treatment decreased the levels of serum β-CTX in both postmenopausal women and OVX mice. In the clinical trial, the MMF wearable device mitigated the decrease in P1NP levels compared to the control group, a trend consistent with the increase in serum P1NP levels observed in OVX mice following MMF exposure. The improvement in bone turnover induced by the decreased of β-CTX levels and the relative increased of P1NP may contribute to the beneficial effects of MMF wearable device not only on the lumbar spine's aBMD (exposed region) but also on the aBMD of total hip and femoral neck (non-exposed region) in participants. However, for another bone formation marker, OCN, MMF exposure did not significantly increase its serum levels in mice, even reduced serum OCN levels compared to the control group in clinical trials. This may be attributed to the inhibitory effect of MMF on osteoclast activity, as the circulating levels of biologically active OCN are regulated by osteoclasts. During the bone resorption process, the acidic environment created by osteoclasts leads to the conversion of inactive c-carboxylated osteocalcin (GlaOCN) to active undercarboxylated osteocalcin (GluOCN) [26]. The increased of osteoclast activity in mice resulted in elevated levels of GluOCN in the serum, and impaired osteoclast function could decreased the GluOCN level [27]. Regarding the fact that MMF exposure did not change serum OCN levels in OVX mice but decreased them in PMOP patients compared to their respective controls, which may be attributed to differences in MMF exposure patterns between animal and clinical study. It is worth noting that the clinical trial involved localized exposure to a MMF in the lumbar spine region, whereas in the animal experiment, mice were whole-body exposed to MMF. Furthermore, there are metabolic differences between mice and humans.

In this study, we also have investigated the correlation between age and BMD changes among participants in different groups. The results showed that there was minimal correlation between age and lumbar spine BMD changes in the control group. However, there was a negative correlation between lumbar spine BMD changes and age in MMF group, although no statistically significant. This suggests that MMF is more effective in improving BMD in younger PMOP patients. With the bone undergoes aging, the sensitivity of bone to mechanical stimuli was reduced gradually [28]. All subjects in SMFs are subject to the action of magnetic force, which is one of the primary mechanisms SMF biological effects [29,30]. Therefore, the relationship between the effects of MMF on PMOP patients with different ages and the magnetic force deserves further research. Additionally, in the early postmenopausal period, the reduction in estrogen levels leads to rapid bone loss, with an annual bone loss rate of 3–5%. This accelerated bone loss can persist for 5–10 years and primarily affects trabecular bone. In the late postmenopausal period, the rate of bone loss slows down, and cortical bone loss becomes more predominant, and associated with an increased risk of fragility fractures [4].

Considering the significant regulatory effect of MMF on bone remodeling in the present study, it is possible that MMF may have a more pronounced therapeutic effect on bone in a period of rapid bone loss with high bone turnover. In the future, it would be interesting to include participants from different age groups to study the effects of MMF exposure on BMD at different stages of aging.

PMOP patients usually suffer from low back pain [31–33]. Various studies indicated that SMFs had an analgesic effects [34]. Suzan et al. found that 20 mT MMF exposure had a positive effect on patients with chronic lumbar radicular pain [35]. Studies indicated that the relief of chronic lumbar radicular pain by the SMF was associated with the magnetic field intensity [36,37]. In this study, we found that 6 hour per day MMF treatment effectively alleviated low back pain in PMOP patients. This may be attributed to the regulatory effects of MMFs on neural signal transduction and the release of inflammatory factors. Additionally, studies have shown that SMF exposure can influence orientation during the bone formation process [38]. Therefore, although 90 days of MMF treatment did not significantly increase the aBMD of the lumbar spine in participants, its modulation of bone turnover may have improved the microstructure and stability of the lumbar spine, potentially contributing to the alleviation of low back pain. Furthermore, due to the inconsistency of conclusions derived from a multitude of SMF treatments with varying intensities and exposure durations, further research is warranted to explore the relationship between the dosage of SMF exposure and its impact on osteoporosis and related pain.

However, this study still has several limitations. Firstly, the lack of in-depth mechanistic research. This is because the aim of this study primarily focused on exploring the clinical efficacy of MMF in treating PMOP. Our previous studies have demonstrated that SMFs regulated cellular and systemic iron metabolism, which is closely associated with osteoporosis [39–42]. Therefore, we will investigate the mechanisms of MMF therapy for PMOP based on iron metabolism in subsequent studies. Secondly, the sample size in the clinical trial was relatively small, and the participants' characteristics were not comprehensively assessed, including factors such as dietary and exercise habits. Since there were no clinical reference data on MMF for the treatment of osteoporosis, the initial intention of designing this clinical trial was to explore the therapeutic effects of MMF on PMOP using a small sample size as a preliminary investigation. Although the valid data obtained in this clinical trial met the minimum sample size required by the study design, the withdrawal of 8 cases resulted in a reduced final sample size, which may still reduce the statistical significance of differences between treatment groups. Incorporating more comprehensive participant characteristics would help assess the robustness of the experimental results through sensitivity analysis and enhance the understanding of the relationship between the effects of MMF on PMOP and participants' characteristics. Surprisingly, we found that MMF effectively regulated bone turnover, alleviated low back pain, and exhibited a tendency to increase lumbar spine BMD. Thirdly, the clinical trial in this study had only a single endpoint, and the trial duration was limited to 90 days, which is relatively short for observing the effects of MMF, a mild intervention, on bone mineral density. The long-term therapeutic effects of MMF on osteoporosis or the potential long-term effects after MMF treatment cessation remain unclear. Therefore, multicenter, large-scale randomized RCTs with longer durations and multiple time points are necessary to comprehensively evaluate the therapeutic effects of MMF on osteoporosis. Furthermore, in this study, we have only investigated the effects of lumbar spine local MMF exposure on BMD and BTMs in PMOP patients. Therefore, further investigation is needed to explore the effects of whole-body MMF exposure or localized MMF exposure at other sites, such as the hip, on osteoporosis.

In conclusion, the MMF exposure not only improved the bone microstructure and bone remodeling homeostasis in OVX mice but also significantly enhanced the bone mechanical properties. The results from RCT demonstrated that 90-day MMF treatment significantly improved serum BTMs and relieved low back pain in PMOP patients. Furthermore, MMF treatment exhibited a positive effect on BMD of the lumbar spine in PMOP patients. It indicated that MMF is a potential adjuvant therapy for osteoporosis and will promote the clinical translation research and application of SMFs.

Supporting Information

S1 Data. Supplementary material.
(DOCX)

S1 Checklist. CONSORT 2010 checklist of information to include when reporting a randomised trial*.
(DOC)

S1 Protocol. Trial protocol in English.
(DOCX)

Author contributions

Conceptualization: Shenghang Wang, Xiaosu Bai, Min Wei, Hao Zhang, Peng Shang.

Data curation: Shenghang Wang, Jiancheng Yang, Yunpeng Wei, Chao Cai, Shuai Chen, Youde Wu, Xiao Li, Lilei Sun, Xianglin Li, Ming Gong, Jianhua Zhou, Yawei Hu, Wang Zhang, Zengfeng Guo, Jiacheng Liao, Chunling Luo, Yanwen Fang, Hao Zhang.

Formal analysis: Shenghang Wang, Ting Huyan, Hao Zhang.

Funding acquisition: Shenghang Wang, Peng Shang.

Investigation: Shenghang Wang, Jiancheng Yang, Yunpeng Wei, Shuai Chen, Xiao Li, Lilei Sun, Xianglin Li, Ming Gong, Jianhua Zhou, Yawei Hu, Zengfeng Guo, Jiacheng Liao, Chunling Luo, Ting Huyan, Yanwen Fang, Hao Zhang.

Methodology: Shenghang Wang, Jiancheng Yang, Yunpeng Wei, Chao Cai, Youde Wu, Wang Zhang, Jiacheng Liao, Chunling Luo, Xiaosu Bai, Xinle Luo, Zhouqi Yang, Peng Shang.

Project administration: Zhouqi Yang, Min Wei.

Resources: Hao Zhang, Peng Shang.

Software: Jiancheng Yang, Liming Duan.

Supervision: Jiancheng Yang, Jiacheng Liao, Chunling Luo, Xiaosu Bai, Liming Duan, Min Wei, Yanwen Fang, Peng Shang.

Writing – original draft: Shenghang Wang, Jiancheng Yang.

Writing – review & editing: Hao Zhang, Peng Shang.

References

1. Compston JE, McClung MR, Leslie WD. Osteoporosis. Lancet. 2019;393(10169):364–76.
2. Song S, et al. Advances in pathogenesis and therapeutic strategies for osteoporosis. Pharmacol Ther 2022;237:108168.
3. van Staa TP, et al. Epidemiology of fractures in England and Wales. Bone 2001;29(6):517–22.
4. Eastell R, O'Neill TW, Hofbauer LC, Langdahl B, Reid IR, Gold DT, et al. Postmenopausal osteoporosis. Nat Rev Dis Primers. 2016;2:16069. https://doi.org/10.1038/nrdp.2016.69 PMID: 27681935
5. Khosla S, Hofbauer LC. Osteoporosis treatment: recent developments and ongoing challenges. Lancet Diabetes Endocrinol. 2017;5(11):898–907. https://doi.org/10.1016/S2213-8587(17)30188-2 PMID: 28689769
6. Reid IR, Billington EO. Drug therapy for osteoporosis in older adults. Lancet. 2022;399(10329):1080–92. https://doi.org/10.1016/S0140-6736(21)02646-5 PMID: 35279261
7. Cosman F, Crittenden DB, Adachi JD, Binkley N, Czerwinski E, Ferrari S, et al. Romosozumab treatment in postmenopausal women with osteoporosis. N Engl J Med. 2016;375(16):1532–43. https://doi.org/10.1056/NEJMoa1607948 PMID: 27641143
8. Zhang W, Luo Y, Xu J, Guo C, Shi J, Li L, et al. The Possible role of electrical stimulation in osteoporosis: a narrative review. Medicina (Kaunas). 2023;59(1):121. https://doi.org/10.3390/medicina59010121 PMID: 36676745
9. Bassett CA, Pilla AA, Pawluk RJ. A non-operative salvage of surgically-resistant pseudarthroses and non-unions by pulsing electromagnetic fields. A preliminary report. Clin Orthop Relat Res. 1977;124:128–43.

10. Catalano A, Loddo S, Bellone F, Pecora C, Lasco A, Morabito N. Pulsed electromagnetic fields modulate bone metabolism via RANKL/OPG and Wnt/β-catenin pathways in women with postmenopausal osteoporosis: A pilot study. Bone. 2018;116:42–6. https://doi.org/10.1016/j.bone.2018.07.010 PMID: 30010081

11. Bassett CA, Pawluk RJ, Pilla AA. Acceleration of fracture repair by electromagnetic fields. A surgically noninvasive method. Ann N Y Acad Sci. 1974;238:242–62.

12. Chen G, Zhuo Y, Tao B, Liu Q, Shang W, Li Y, et al. Moderate SMFs attenuate bone loss in mice by promoting directional osteogenic differentiation of BMSCs. Stem Cell Res Ther. 2020;11(1):487. https://doi.org/10.1186/s13287-020-02004-y PMID: 33198804

13. Degen IL, Stetsula VI. Consolidation of bone fragments in a constant magnetic field. Ortop Travmatol Protez. 1971;32(9):45–8. PMID: 5138724

14. Wang S, et al. Safety of exposure to high static magnetic fields (2 T-12 T): a study on mice. Eur Radiol 2019;29(11):6029–37.

15. Dini L, Abbro L. Bioeffects of moderate-intensity static magnetic fields on cell cultures. Micron. 2005;36(3):195–217. https://doi.org/10.1016/j.micron.2004.12.009 PMID: 15725590

16. Yang J, Feng Y, Li Q, Zeng Y. Evidence of the static magnetic field effects on bone-related diseases and bone cells. Prog Biophys Mol Biol. 2023;177:168–80. https://doi.org/10.1016/j.pbiomolbio.2022.11.006 PMID: 36462638

17. Wang S, Liu Y, Lou C, Cai C, Ren W, Liu J, et al. Moderate static magnetic field promotes fracture healing and regulates iron metabolism in mice. Biomed Eng Online. 2023;22(1):107. https://doi.org/10.1186/s12938-023-01170-3 PMID: 37968671

18. Aydin N, Bezer M. The effect of an intramedullary implant with a static magnetic field on the healing of the osteotomised rabbit femur. Int Orthop. 2011;35(1):135–41. https://doi.org/10.1007/s00264-009-0932-9 PMID: 20062989

19. Bruce GK, Howlett CR, Huckstep RL. Effect of a static magnetic field on fracture healing in a rabbit radius. Preliminary results. Clin Orthop Relat Res. 1987;222:300–6.

20. Yang J, Zhou S, Wei M, Fang Y, Shang P. Moderate static magnetic fields prevent bone architectural deterioration and strength reduction in ovariectomized mice. IEEE Trans Magn. 2021;57(7):1–9. https://doi.org/10.1109/tmag.2021.3072148

21. Scott J, Huskisson EC. Graphic representation of pain. Pain. 1976;2(2):175–84. https://doi.org/10.1016/0304-3959(76)90113-5 PMID: 1026900

22. Andreopoulou P, Bockman RS. Management of postmenopausal osteoporosis. Annu Rev Med. 2015;66:329–42. https://doi.org/10.1146/annurev-med-070313-022841 PMID: 25386933

23. Händel MN, Cardoso I, von Bülow C, Rohde JF, Ussing A, Nielsen SM, et al. Fracture risk reduction and safety by osteoporosis treatment compared with placebo or active comparator in postmenopausal women: systematic review, network meta-analysis, and meta-regression analysis of randomised clinical trials. BMJ. 2023;381:e068033. https://doi.org/10.1136/bmj-2021-068033 PMID: 37130601

24. Morley J, Moayyeri A, Ali L, Taylor A, Feudjo-Tepie M, Hamilton L, et al. Persistence and compliance with osteoporosis therapies among postmenopausal women in the UK Clinical Practice Research Datalink. Osteoporos Int. 2020;31(3):533–45. https://doi.org/10.1007/s00198-019-05228-8 PMID: 31758206

25. Hiligsmann M, Cornelissen D, Vrijens B, Abrahamsen B, Al-Daghri N, Biver E, et al. Determinants, consequences and potential solutions to poor adherence to anti-osteoporosis treatment: results of an expert group meeting organized by the European Society for Clinical and Economic Aspects of Osteoporosis, Osteoarthritis and Musculoskeletal Diseases (ESCEO) and the International Osteoporosis Foundation (IOF). Osteoporos Int. 2019;30(11):2155–65. https://doi.org/10.1007/s00198-019-05104-5 PMID: 31388696

26. Han Y, Author2 F, Author3 F, Author4 F, Author5 F. Paracrine and endocrine actions of bone-the functions of secretory proteins from osteoblasts, osteocytes, and osteoclasts. Bone Research. 2018;6:16.

27. Lacombe J, Karsenty G, Ferron M. In vivo analysis of the contribution of bone resorption to the control of glucose metabolism in mice. Mol Metab. 2013;2(4):498–504. https://doi.org/10.1016/j.molmet.2013.08.004 PMID: 24327965

28. Pignolo RJ. Aging and bone metabolism. Compr Physiol. 2023;13(1):4355–86.

29. Zhang B, Yuan X, Lv H, Che J, Wang S, Shang P. Biophysical mechanisms underlying the effects of static magnetic fields on biological systems. Prog Biophys Mol Biol. 2023;177:14–23. https://doi.org/10.1016/j.pbiomolbio.2022.09.002 PMID: 36240898

30. Berry MV, Geim AK. Of flying frogs and levitrons. Eur J Phys. 1997;18(4):307–13. https://doi.org/10.1088/0143-0807/18/4/012

31. Fujimoto K, Inage K, Orita S, Yamashita M, Abe K, Yamagata M, et al. The nature of osteoporotic low back pain without acute vertebral fracture: A prospective multicenter study on the analgesic effect of monthly minodronic acid hydrate. J Orthop Sci. 2017;22(4):613–7. https://doi.org/10.1016/j.jos.2017.01.022 PMID: 28284540

32. Ohtori S, Akazawa T, Murata Y, Kinoshita T, Yamashita M, Nakagawa K, et al. Risedronate decreases bone resorption and improves low back pain in postmenopausal osteoporosis patients without vertebral fractures. J Clin Neurosci. 2010;17(2):209–13. https://doi.org/10.1016/j.jocn.2009.06.013 PMID: 20044258

33. Knezevic NN, Candido KD, Vlaeyen JWS, Van Zundert J, Cohen SP. Low back pain. Lancet. 2021;398(10294):78–92. https://doi.org/10.1016/S0140-6736(21)00733-9 PMID: 34115979

34. Fan Y, et al. The analgesic effects of static magnetic fields. Bioelectromagnetics. 2021;42(2):115–27.

35. Khoromi S, Blackman MR, Kingman A, Patsalides A, Matheny LA, Adams S, et al. Low intensity permanent magnets in the treatment of chronic lumbar radicular pain. J Pain Symptom Manage. 2007;34(4):434–45. https://doi.org/10.1016/j.jpainsymman.2006.12.008 PMID: 17618081

36. László JF, Farkas P, Reiczigel J, Vágó P. Effect of local exposure to inhomogeneous static magnetic field on stomatological pain sensation - a double-blind, randomized, placebo-controlled study. Int J Radiat Biol. 2012;88(5):430–8. https://doi.org/10.3109/09553002.2012.661916 PMID: 22288770

37. Eccles NK. A critical review of randomized controlled trials of static magnets for pain relief. J Altern Complement Med. 2005;11(3):495–509.

38. Kotani H, Kawaguchi H, Shimoaka T, Iwasaka M, Ueno S, Ozawa H, et al. Strong static magnetic field stimulates bone formation to a definite orientation in vitro and in vivo. J Bone Miner Res. 2002;17(10):1814–21. https://doi.org/10.1359/jbmr.2002.17.10.1814 PMID: 12369785

39. Dong D, Yang J, Zhang G, Huyan T, Shang P. 16 T high static magnetic field inhibits receptor activator of nuclear factor kappa-B ligand-induced osteoclast differentiation by regulating iron metabolism in Raw264.7 cells. J Tissue Eng Regen Med. 2019;13(12):2181–90. https://doi.org/10.1002/term.2973 PMID: 31622531

40. Yang J, Zhang J, Ding C, Dong D, Shang P. Regulation of osteoblast differentiation and iron content in MC3T3-E1 cells by static magnetic field with different intensities. Biol Trace Elem Res. 2018;184(1):214–25. https://doi.org/10.1007/s12011-017-1161-5 PMID: 29052173

41. Zhang G, et al. 1-2 T static magnetic field combined with Ferumoxytol prevent unloading-induced bone loss by regulating iron metabolism in osteoclastogenesis. J Orthop Translat, 2023;38:126–140.

42. Lv H, Wang Y, Zhen C, Liu J, Chen X, Zhang G, et al. A static magnetic field improves bone quality and balances the function of bone cells with regulation on iron metabolism and redox status in type 1 diabetes. FASEB J. 2023;37(7):e22985. https://doi.org/10.1096/fj.202202131RR PMID: 37249350